Mechanical Properties of Composites Reinforced with Recycled Paper and Pine Needles Using Polymer Matrices Containing 50 to 70% Dammar Resin

Cosmin Mihai Miriţoiu [a,*] Adrian Sorin Roşca [b] and Dragoş Tutunea [b]

The main objective of this study was to manufacture and test environmentally friendly composite materials using biomass residues as reinforcement: pine needles and recovered paper. A mixed matrix was also used, with natural dammar resin as the predominant component, in order to favor the eco-friendly nature of the resulting material. The manufacturing process employed was the lay-up hand technique. Another objective was to investigate how dammar resin influences the mechanical properties as its mass percentage increases in the mixed resin composition. To investigate the influence of dammar resin on the mechanical properties of the composites, additional materials were fabricated for comparison, using the same reinforcements but with two types of synthetic matrices: epoxy and acrylic. The samples were tested for tensile strength, compression, bending, Shore D hardness, and vibrations. The results indicated that as the percentage of dammar in the matrix increased, a decrease in the strength and rigidity of the material occurred, accompanied by an increase in elasticity and ductility. Water absorption tests showed that the saturation process occurred much faster, as pine needles tend not to absorb a significant amount of water due to the presence of lignin, wax, resins, and pectin, which act as a natural water-repellent barrier.

DOI: 10.15376/biores.20.2.3884-3909

Keywords: Pine needles; Dammar resin; Bio-based resin; Mechanical properties

Contact information: a: University of Craiova, Faculty of Mechanics, Department of Applied Mechanics and Civil Constructions, Craiova, Romania; b: University of Craiova, Faculty of Mechanics, Department of Vehicles, Transports and Industrial Engineering, Craiova, Romania;
** Corresponding author: miritoiucosmin@yahoo.com*

INTRODUCTION

Biomass, derived from plant materials and animal waste, serves as a renewable energy source. Predominantly sourced from plants and organic residues, it is promoted as a sustainable alternative to fossil fuels, aiding in greenhouse gas reduction. Bioenergy is produced through combustion, biofuel conversion, or anaerobic digestion for biogas. However, its environmental impact depends on biomass harvesting and processing methods, making sustainable resource management crucial for balancing energy demand and ecosystem protection (Houghton 2008; IPCC 2011).

Dammar resin, which was sourced from Dipterocarpaceae trees native to East Asia, has been widely studied (see for example Abdel-Ghani *et al.* 2009; Mittal *et al.* 2010). It is mainly used in paper production, wood coatings, and as a drawing pigment (see for example Bonaduce *et al.* 2013; La Nasa *et al.* 2014). The composition of dammar resin has

been thoroughly investigated. Studies by Topp and Pepper (1949), Clearfield (2000), and Mittal *et al.* (2010) highlighted key constituents, such as polycaninene (a polymeric component), β-resene (alcohol-insoluble), and α-resene (soluble). It also contains small amounts of C15 sesquiterpenes and is primarily made up of tetracyclic dammarane structures, along with oleanane, ursane, and hopane-type pentacyclic compounds (Mirițoiu 2024). Applications of dammar in mixed matrices have been explored by Stănescu (2015), Mirițoiu *et al.* (2020), Franz *et al.* (2021), and Ciucă *et al.* (2022), who examined both its chemical profile and mechanical performance when blended with synthetic resins. Results showed that higher dammar content reduces the mechanical strength of such formulations.

Pine needles are a biomass component rich in cellulose (52 to 60%), hemicellulose (20%), lignin (13 to 15%), and various extractives (Alzebdeh *et al.* 2019; Cogurcu 2022). In summer, fallen pine needles form a dense, acidic layer on the forest floor, reducing soil water retention and limiting plant diversity (Vestgarden *et al.* 2004; Soong *et al.* 2015). Their slow degradation, due to lignocellulosic complexity and microbial communities, further impacts ecosystems (Maleki *et al.* 2017). Additionally, their high flammability increases wildfire risks, leading to vegetation loss, soil erosion, and long-term nutrient depletion (Singha and Thakur 2008). Uncontrolled accumulation can harm biodiversity and forest stability (Third Pole 2017; Rana *et al.* 2023).

The state of Uttarakhand, India, has approximately 343 thousand hectares of pine forests, generating around 250 thousand tons of dry biomass annually, which holds potential for energy, agriculture, and industry. Pine straw production varies by region, influenced by climate and soil conditions (Bisht and Thakur 2020; Rana *et al.* 2023). In the southeastern USA, yields range from 650 to 725 bales per acre annually (see Dickens *et al.* 2020), while Texas produces about 300 bales (Taylor and Foster 2004; Dyer *et al.* 2012). Florida averages 500 bales (see Duryea 1989), and North and South Carolina yield around 280 bales (see Rana *et al.* 2023), with coastal South Carolina reaching 260 bales per acre (see Gresham 1982). These variations highlight the need for optimized forest management and sustainable reuse of pine needle material.

Pine needles have various applications across agriculture, energy, construction, and medicine. They serve as animal bedding, absorbing moisture and reducing odors, and as a fuel source for fire ignition (Flemingfarm 2017; Azmat 2024; Kingsbury 2025). In construction, their fibers reinforce bricks, improving strength and durability. In India, a 100 to 150 kW power plant generates electricity from pine needle material (Khan 2012), while charcoal from pine needles offers a sustainable fuel alternative (Khuller 2019). Research conducted by Gosh and Gosh (2011), Asghar *et al.* (2014), Gupta and Mondal (2021), Gupta *et al.* (2022), and Xie *et al.* (2022) has explored their use in lactic acid fermentation, essential oil extraction, and biofuel production through pyrolysis, optimizing efficiency with advanced modeling techniques. Pretreatment methods enhance their potential for renewable energy, increasing methane production by 21.4% (Mahajan *et al.* 2020). Additionally, pine needles act as bioindicators of air pollution and are used in medicinal formulations (Klánová *et al.* 2009; Likus-Cieślik *et al.* 2020; Chung *et al.* 2021; Koutsaviti *et al.* 2021; Zsigmond *et al.* 2021; Guo *et al.* 2022).

Another use of pine needles has been their application as a reinforcement in the manufacturing of composite materials. Pine needle fibers have been used as reinforcement in combination with various types of polymers and resins for the development of composite materials. These include polypropylene, which provides good mechanical strength and flexibility (see for example Malkapuram *et al.* (2010) or Alzebdeh *et al.* (2019)), and polylactic acid, a biopolymer commonly used in eco-friendly applications (see for example

Sinha *et al.* (2018) or Operato *et al.* (2023)). Additionally, pine needle fibers have been incorporated into resin matrices, such as epoxy resin, which is known for its superior adhesion and chemical stability (see for example Gairola *et al.* (2019)), and urea-formaldehyde resin, which is widely used in the wood and adhesive industries (see for example Singha and Thakur (2008) or Thakur *et al.* (2013)). Other resins used in combination with pine needle fibers include phenol-formaldehyde, resorcinol-formaldehyde, and urea–resorcinol–formaldehyde, each contributing to enhanced mechanical and thermal properties of the resulting composite materials (see for example Singha and Thakur (2008), Thakur and Singha (2011), or Singha and Jyoti (2013)). This utilization of pine needle fibers in composites enables the production of materials with improved strength, reduced weight, and increased sustainability, making them suitable for applications in the automotive industry, construction, packaging, and many other fields. In the study by Dinesh and Kim (2023), pine needle fibers (PNFs) were incorporated as a reinforcing element in the thermoplastic elastomer styrene-ethylene-butylene-styrene (SEBS) matrix. Through utilizing a maleic anhydride-grafted SEBS compatibilizer, the goal was to develop environmentally friendly and cost-effective PNF/SEBS composites. This approach supported the creation of sustainable materials with applications across various industries (see Dinesh and Kim (2023)). A cradle-to-gate Life Cycle Analysis study was conducted by Operato *et al.* (2023) on eco-friendly polylactic acid (PLA) composites reinforced with 10 to 40 vol% lignocellulosic fibers from pine needles (PN) or kenaf (KB). The assessment covered raw material sourcing, transportation, fiber processing, melt compounding, and granulation to produce PLA/PN and PLA/KB bio-pellets. Findings revealed a significantly lower environmental impact compared to pure PLA, with benefits increasing with fiber content (*e.g.*, a 48% reduction in greenhouse gas emissions and a 32% decrease in primary energy demand for composites with 40% fiber). Additionally, enhanced mechanical properties allow for material savings, reducing weight by up to 8% at 30% KB while maintaining structural performance. Gupta *et al.* (2023) explored a cleaner technology using a combined approach: a mild 1% $Ca(OH)_2$ treatment followed by *Phanerochaete chrysosporium* (a laccase-producing fungus) applied to a mixture of paddy straw and pine needles to obtain cellulose-rich pulp for biodegradable paper production. Scanning electron microscopy (SEM) and Fourier transform infrared (FTIR) analyses revealed a denser cellulose network and –OH bonds compared to alpha-cellulose. The best pulp (Kappa no. 24, SR 59) was used to produce biodegradable paper sheets of various GSM types (40, 50, 75, and 100 GSM), with mechanical properties evaluated. The 100 GSM sheets showed the highest tensile strength (110 Nm/g) and Cobb index (345.77 g/m^2), comparable to standard corrugated sheets. Mengual *et al.* (2017) produced thermo-compressed plates using pine needles (powder and fiber) and natural resins (ELO and GREENPOXY). After mechanical characterization, the optimal combination was selected, and sandwich panels based on balsa wood and cork were fabricated for further evaluation. The best results were achieved using GREENPOXY resin and boat wood, with the choice between micronized pine or fiber depending on industrial needs.

The pine needle structure in composites has also been used for the fabrication of other materials while maintaining their alignment. In the research made by Fu *et al.* (2022), highly aligned ZnO nanorods were epitaxially grown on electrospun poly vinylidene fluoride nanofibers, resulting in ZnO@PVDF composite nanofibers with a pine-needle-like biomimetic structure. The nanofibers were characterized before and after the hydrothermal reaction using SEM, FTIR, X-ray diffraction (XRD), and piezoelectric analysis. Results showed that controlling hydrothermal parameters, including the

$ZnCl_2$/HTMA ratio, ammonium hydroxide volume, reaction time, and temperature, is crucial for optimizing ZnO nanorod microstructure and piezoelectric performance.

Beyond their use as reinforcement in composite materials, efforts have also been made to incorporate pine needles into concrete. Studies have shown that pine needle fibers can enhance compressive strength, splitting strength, and modulus of rupture, while also improving ductility and toughness (see for example Long and Wang (2021) or Wang and Long (2021)). These findings suggest the potential of pine needle fibers in developing a novel plant-fiber-reinforced concrete composite. Additionally, research from Cogurcu (2022) has found that pine needles can improve strength and crack resistance without compromising the material's self-compacting properties. Strzałkowski *el al.* (2024) indicate that mortars containing both 1.5% and 2.5% bio-powder from lavender and black pine waste exhibit strong bactericidal properties, lower moisture absorption at high air humidity, reduced thermal conductivity, and a 22 to 27% decrease in compressive strength. Additionally, no significant impact was observed on flexural strength, while a considerable reduction in capillary action was noted under both short-term and long-term water exposure conditions.

In this study, composite materials were manufactured using two types of residues: paper and pine needles. Several bio-based matrices, predominantly composed of natural dammar resin, were used for the composites. The proportion of natural dammar resin was varied between 50% and 70% in the composition of the bio-based resins. This resin originates from India and is extracted from the *Dipterocarpaceae* family of trees (see Mittal *et al.* (2010)). Additionally, two fully synthetic matrices (epoxy Resoltech 1050 with hardener 1058s and acrylic ClarocitKit with its corresponding hardener) were also used to assess the influence of dammar resin on the mechanical properties, compared to samples made exclusively from synthetic matrix materials. The amount of reinforcing material used was 60% (30% paper and 30% pine needles), while the remaining 40% was the matrix. It can be said that the present work is a continuation of the research conducted in Miritoiu (2024), which aims to find ways to reuse waste materials for the fabrication of composite materials.

EXPERIMENTAL

Materials

Various matrix formulations and reinforcing fibers were used to fabricate the composite materials. The matrices included synthetic resins, such as epoxy Resoltech 1050 and acrylic Clarocit, alongside bio-based matrices that combined natural dammar resin with a small proportion of synthetic resins to enhance the polymerization process. The dammar resin, sourced from Shorea trees of the Dipterocarpaceae family, was obtained from a local supplier (Foita de Aur (2023)). The synthetic epoxy resin was purchased from a local supplier (Polydis 2023). The synthetic acrylic resin was purchased from a local supplier (Struers 2023). The technical specifications of the synthetic resins are available on the manufacturers' websites: Resoltech 1050 (2023) provides details for the epoxy resin, while Clarocit Kit (2023) covers the acrylic variant. The reinforcement consisted of recovered paper and pine needle residues, which were arranged side-by-side to form a structured layer (as illustrated in Fig. 1a). To prepare the dammar resin for use, it was liquefied by immersion in turpentine and subsequently stored in sealed containers. A

comprehensive list of all resins utilized in this study, along with their corresponding abbreviations, is provided in Table 1.

Table 1. Matrices Used for Composite Materials

Criteria Number	Mass Percentage of the Epoxy Resin Resoltech 1050 (%)	Mass Percentage of the Dammar Resin (%)	Abbreviation
1	100	0	E100
2	50	50	HE50
3	40	60	HE40
4	30	70	HE30
Criteria Number	Mass Percentage of Acrylic Resin Clarocit (%)	Mass Percentage of the Dammar Resin (%)	Abbreviation
5	100	0	A100
6	50	50	HA50
7	40	60	HA40
8	30	70	HA30

The mechanical and chemical properties of this type of bio-based resin have been previously studied by Stănescu (2015), Mirițoiu *et al*. (2020), Franz *et al*. (2021), and Ciucă *et al*. (2022). These investigations focused on a detailed analysis of mechanical behavior (tensile strength, dynamic behavior through free vibrations, Shore D hardness, *etc*.) as well as chemical properties (FTIR analysis, energy dispersive spectroscopy analysis, *etc*.). As the percentage of dammar resin in the matrix structure increases, the mechanical properties are affected (strength and elastic modulus decrease significantly, while plasticity increases). The percentages presented in Table 1 (namely, a maximum of 70% natural dammar resin) were chosen because other studies have shown that exceeding this percentage in the matrix leads to a decrease in strength by approximately 3.5 times and in the elastic modulus by about 6 times, compared to the case in which dammar resin is not present in the matrix (see, for example, Franz *et al.* (2021)).

Methods

For the manufactured composite materials, a combination of recovered paper and pine needles was used as the reinforcing material. The reinforcement process was carried out using the hand-layup technique in successive layers. Initially, a thin layer of resin was applied with a brush onto a normal office sheet of paper IQ Economy+ with a mass per unit area of 80 g/m², which was purchased from a local supplier (see IQ Economy+ (2024)). Then, the pine needles were carefully arranged side by side over the resin layer. The pine needles were collected in February 2024 from the Baia de Fier area, Gorj County, Romania. They were brought to the laboratory and kept at room temperature until June, when sample fabrication began. No thermal or chemical treatment was applied to the pine needles, and they were not fully dried. As shown in Fig. 1, the needles retained their green color at the time of casting. The purpose of applying the resin was to secure and ensure the adhesion of the pine needles to the paper surface. This resulted in a reinforced lamina. The same method was repeated for nine additional laminae, resulting in a layered composite material. To obtain a specific type of material, a thin layer of resin was applied to each lamina, then they were stacked and pressed under a mass of 300 kg, evenly distributed over an area of 420 × 297 mm². To allow full polymerization, specimens with synthetic resin were trimmed after five days, whereas those made with bio-based resins were processed after ten days. Until the specimens were trimmed, pressure under a 300 kg weight was maintained

consistently each day. The weight was removed on the day the specimens were cut. An example with the final plate obtained with one of the H type resins mentioned in the Table 1 is presented in Fig. 2.

Fig. 1. A detail with the final shape of a lamella with pine needles placed on a paper waste support

Fig. 2. An example of a plate with HE40 resin reinforced with pine needles trash and paper waste

Fig. 3. An example with 15 samples from a plate with HE40 resin used for the tensile test

Because the produced materials will be subjected to a variety of destructive and non-destructive evaluations, including tensile, compressive, bending, vibration tests, Shore D hardness measurement, and water absorption assessment, they will be designated by abbreviations to ensure easier identification in the text. The compilation of abbreviations used in the following sections has been presented in Table 2.

Table 2. Symbols Used for Samples

The first letter of the sample name is assigned based on the testing method used.	T – tensile test
	C – compression test
	B – bending test
	V – vibration test
	S – Shore D hardness test
	W – water absorption test
The second and third letters of the sample name are determined based on the type of reinforcement used.	P – paper waste (2nd letter)
	P – pine needles trash (3rd letter)
The second-to-last group of letters and numbers in the sample name originates from the resin abbreviations, as presented in Table 1.	H – bio-based resin
	E – epoxy resin
	A – acrylic resin
	100, 50, 40, 30 – percentages of the synthetic resins
The final set of numbers corresponds to the samples tested for tensile, compression, and bending.	The specimen number ranges from 01 to 15, as 15 specimens were tested for each type of material.

Test Standards and Characterizations

Tensile test

For the tensile assessment, plates were molded using paper waste and pine needles trash reinforcements, combined with the eight types of resins specified in Table 1 (two synthetic and six bio-based variants). From each plate, 15 individual specimens were obtained. A representative example of the 15 tensile test specimens cut from the T PPHE40 group is illustrated in Fig. 3. The tensile evaluation followed the ASTM D3039/D3039M-08 (2014) standard, with specimens measuring 250 mm in length, 25 mm in width, and 8 mm in thickness. The tests were conducted using an Instron 1000 HDX (Instron, Norwood, MA, USA) universal testing apparatus.

Compression test

For the compression assessment, plates similar to those used in tensile testing were fabricated, with the distinction that they comprised 19 layers (laminae). The same pressure conditions and duration as those described in the *Methods* section were used. The specimens were cut to dimensions of approximately 15 mm in length, 15 mm in width, and 15 mm in thickness. The compression evaluation was carried out following the guidelines of the ASTM D695-23 (2016) standard. A universal LGB Testing Equipment machine (LGB Testing Equipment, Azzano San Paolo, Italy), equipped with a specialized compression testing fixture, was employed for the experiments. The use of 19 layers ensured sufficient specimen thickness to promote failure through compressive crushing rather than instability due to buckling.

Bending test

For the flexural evaluation, test plates similar to those used for tensile experiments were manufactured, incorporating recycled paper and pine needle fragments as reinforcements, with a matrix consisting of the eight resin types specified in Table 1. The structure maintained the same 10-layer configuration as in the tensile test. From these fabricated plates, 15 specimens were precisely cut to the dimensions of 200 mm in length, 32 mm in width, and 8 mm in thickness. A universal LGB Testing Equipment machine (LGB Testing Equipment, Azzano San Paolo, Italy), equipped with a three-point bending

apparatus, was employed for the testing process. The bending assessment was carried out in compliance with the ASTM D790-17 (2017) standard.

Vibration test

The specimens used in the vibration analysis retained the same dimensions and characteristics as those described in the tensile testing section. Each sample was securely clamped at one end, leaving the opposite end free, where a Bruel&Kjaer accelerometer with a sensitivity of 0.04 pC/ms² was attached. This accelerometer was linked to a Nexus signal conditioning unit, which subsequently transmitted the data to a SPIDER 8(HBK Hottinger Brüel & Kjær, Darmstadt, Germany) acquisition system. The SPIDER 8 device was further connected to a laptop, where the recorded experimental values were stored.

Shore D hardness test

The Shore D hardness assessment was performed in compliance with the ASTM D2240-15 (2017) standard. Specimens with the same dimensions as those outlined in the tensile testing section were used. Five measurements were taken at intervals of 50 mm along the sample's length, with the outermost points positioned 25 mm from each edge. All measurements were conducted at the center of the specimen's width to ensure result consistency.

Water absorption

The water absorption experiment was carried out in accordance with the ASTM D570 (2022) standard. Initially, the specimens were weighed and then submerged in distilled water contained in Berzelius beakers. Each sample measured 76.2 mm in length, 25.4 mm in width, and 8 mm in thickness. After 24 h of immersion, the specimens were removed, and any excess surface water was carefully wiped off using a dry cloth. The samples were then weighed using a SHIMADZU (Kyoto, Japan) analytical balance with a precision of 0.01 g. This weighing procedure was repeated daily until the weight variation between two consecutive days fell below 0.05 g. Finally, the specimens were air-dried at ambient temperature for 72 h, with their final weight recorded daily.

RESULTS AND DISCUSSION

Tensile Test

During the tensile strength assessment, 15 specimens were obtained from each cast plate containing the eight resin types detailed in Table 1. The samples were cut in alignment with the orientation of the pine needles, and the tensile test was carried out along the fiber axis, as shown in Fig. 4.

Fig. 4. An example of how the tensile test force was applied along the fibers

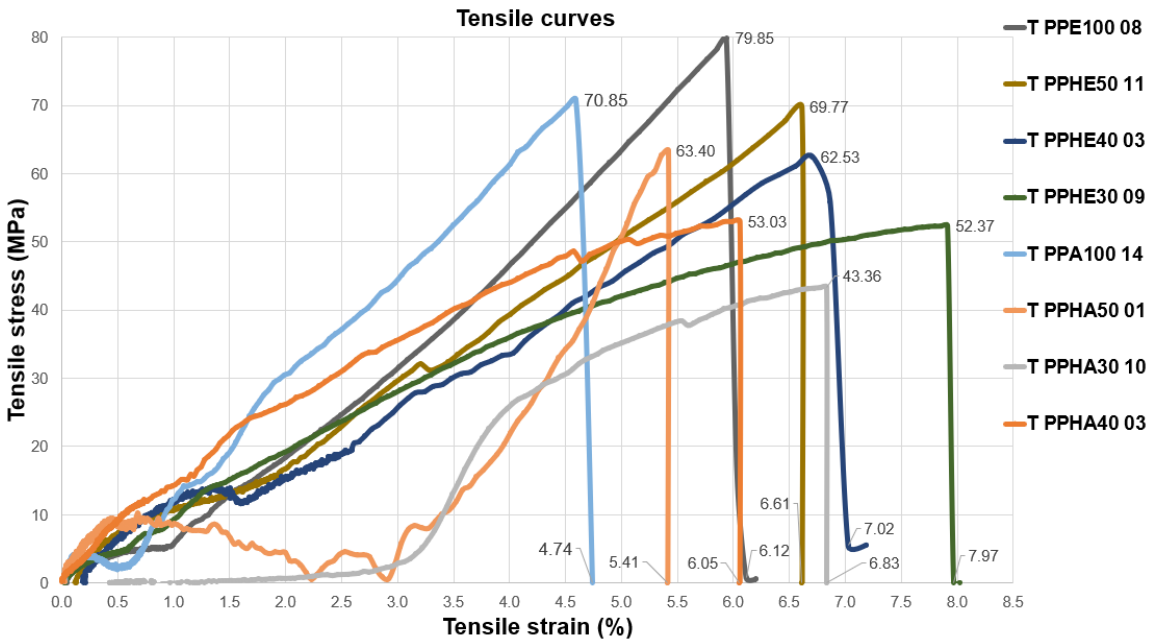

Fig. 5. The stress-strain curves from the tensile tests for all representative samples with matrices composed of all eight types of resins

For each type of material subjected to testing, the arithmetic average of the obtained mechanical properties was calculated, thus providing a reference basis for comparative analysis. There were 15 replicates for each condition. Based on these average values, representative samples were selected, meaning those specimens whose mechanical properties were closest to the arithmetic mean. In the Fig. 5, the characteristic curves corresponding to each type of material were presented, being overlaid on the same graph to allow a clear visualization of variations in mechanical behavior. For example, in the testing of the 15 specimens of type T PPHE50 for tensile strength, specimen 03 was identified as representative due to the proximity of its mechanical properties to the calculated average. Thus, the characteristic curve of this specimen is illustrated in Fig. 5, being used as a reference for the general interpretation of the behavior of this type of material. The presentation of characteristic curves on a common graph not only facilitated the comparison between the analyzed materials but also allowed for the highlighting of the influence of studied variables, such as the modification of the proportion of natural dammar resin or the transition from synthetic epoxy resin to acrylic resin. This approach provided a clear picture of how these changes influenced the mechanical behavior of the materials and helped identify specific trends. In this context, Fig. 5 presents the results of the tensile test for all representative samples, in the form of stress-strain curves, highlighting the differences and similarities between the analyzed materials. This methodology contributed to a deeper understanding of how the composition of materials influenced mechanical performance, thus providing valuable insights for practical applications and the optimization of materials used in various fields.

The tested specimens exhibited tensile strength ranging from 43 to 80 MPa, while elongation at break varied between 4.7% and 8%. It was observed that specimens containing epoxy resin in the matrix composition demonstrated superior mechanical properties compared to those in which acrylic resin was used as a binder. These differences were reflected in higher values for breaking strength and elongation at break in materials

with an epoxy matrix. This result can be explained by the fact that epoxy resin inherently possesses better mechanical characteristics than acrylic resin, providing greater cohesion and a higher resistance capacity to mechanical stresses. The analysis of the tensile curves presented in Fig. 5 indicates a downward trend in tensile strength as the percentage of natural dammar resin increases. This reduction in strength can be attributed to the lower mechanical properties of dammar resin compared to synthetic resins, such as epoxy and acrylic, which provide greater stiffness and internal cohesion to the material. At the same time, data from Fig. 5 highlight an opposite trend concerning elongation at break, which increases with a higher percentage of dammar. This phenomenon can be explained by the more elastic nature of dammar resin compared to synthetic resins, suggesting that materials with a high dammar content become more ductile, exhibiting a greater capacity for deformation before breaking. This characteristic may be advantageous in applications where material flexibility is a key criterion. Furthermore, the arithmetic mean values of the longitudinal modulus of elasticity for each type of material are provided in Table 3.

Table 3. Modulus of Elasticity Arithmetic Mean Values

Material Type	T PPE100	T PPHE50	T PPHE40
Modulus of elasticity *E* (MPa)	4968	4821	4755
Material type	T PPHE30	T PPA100	T PPHA50
Modulus of elasticity *E* (MPa)	4524	4842	4717
Material type	T PPHA40	T PPHA30	
Modulus of elasticity *E* (MPa)	4615	4415	

These values were determined by calculating the arithmetic mean of the results obtained for the 15 tested specimens of each material category. For instance, in the case of T PPHE50 specimens, the modulus of elasticity value was obtained by averaging the results recorded for specimens numbered from T PPHE50 01 to T PPHE50 15. This calculation methodology ensures an accurate and representative assessment of the mechanical behavior of each material type, allowing for a rigorous comparison between different compositions and highlighting the influence of each matrix component on the overall performance of the material. These insights are essential for optimizing material formulations and selecting the most suitable combinations based on the specific requirements of industrial applications. In terms of tensile strength, a 2.1-fold increase was observed compared to the study by Sinha *et al.* (2018). This enhancement can be attributed to the incorporation of paper into the composite formulation, which contributed to the improvement of the material's mechanical properties. With respect to tensile strength, significantly higher values—approximately 2.4 times greater—were also recorded in comparison to the results reported by Singha and Thakur (2010). This improvement can be explained by the addition of paper lamellae into the composite structure, which contributed to the enhancement of tensile resistance properties.

Compression Test

For the compression test, a procedure similar to that used in the tensile test was followed, ensuring a consistent methodology for evaluating the mechanical properties of the materials. From each type of analyzed material, 15 specimens were selected and processed to obtain relevant and representative results. Following the tests, a representative

specimen was identified for each material category, selected based on the proximity of its mechanical characteristics to the arithmetic mean values of the respective material's properties. The characteristic curves obtained from the compression test for these representative specimens are presented in Fig. 6, allowing for a clear comparison of the mechanical behaviors of the different tested materials. This approach facilitates the analysis of the influence of each type of matrix on the overall mechanical response of the material, providing valuable insights for optimizing material composition based on the specific requirements of industrial applications.

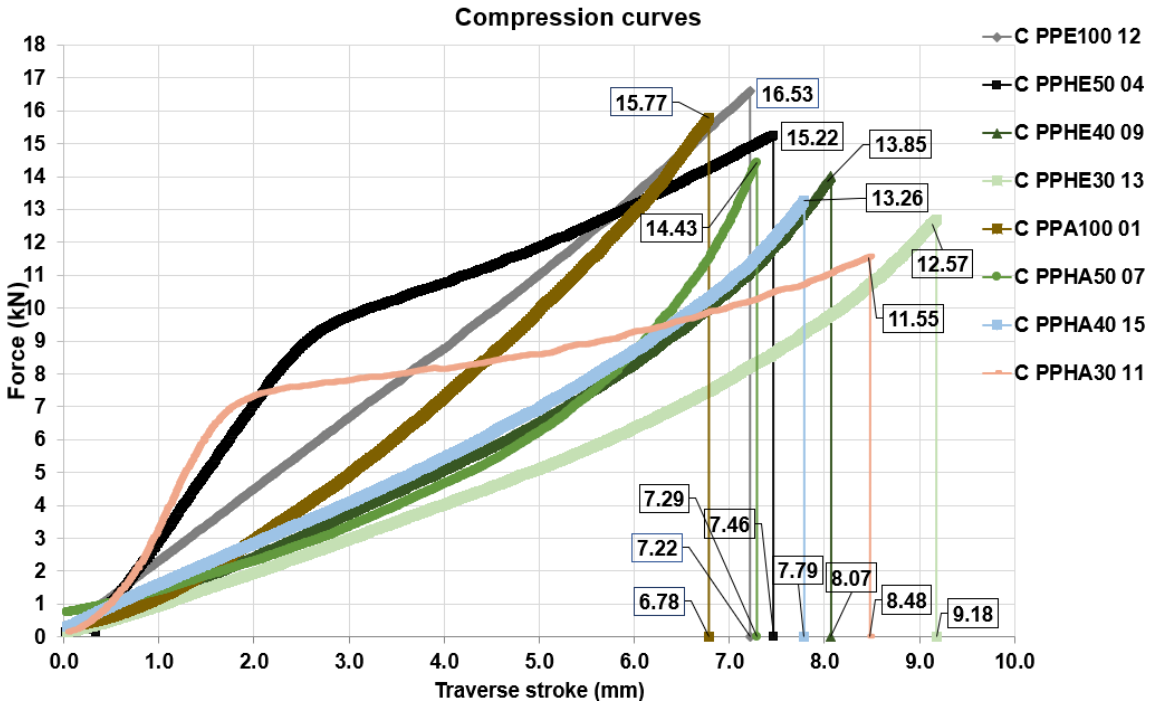

Fig. 6. The force-displacement curves from the compression test for all representative samples with matrices composed of all eight types of resins

The arithmetic mean values of the breaking strength determined from the compression test are presented in Table 4. The analysis of the characteristic curves revealed trends similar to those observed in the tensile test, confirming the influence of the matrix composition on the mechanical behavior of the materials. Specifically, it was noted that as the proportion of natural dammar resin increased, the compression displacement also increased, indicating a greater deformation capacity of the material. At the same time, compressive strength gradually decreased, suggesting a reduction in rigidity and the material's ability to withstand mechanical stresses without experiencing structural failure. Another notable aspect highlighted by the experimental tests was the superior behavior of the specimens that incorporated epoxy resin in the matrix composition compared to those that contained acrylic resin. These specimens exhibited higher compressive strength, indicating an improved capacity to withstand mechanical loads without premature failure. As previously mentioned, this result can be explained by the fact that epoxy resin possesses superior mechanical properties compared to acrylic resin, providing greater cohesion and structural stability to the material. These findings are essential for a better understanding of how different matrix components influence the mechanical performance of materials.

Therefore, adjusting the proportion and type of resin used in the composition can be an effective strategy for optimizing the mechanical characteristics of materials, tailoring them to the specific requirements of industrial applications. This approach enables the development of advanced materials capable of delivering enhanced performance based on the practical needs of various application fields.

Table 4. Arithmetic Mean Values of the Compression Breaking Strength

Sample Type	C PPE100	C PPHE50	C PPHE40	C PPHE30
Stress Values (MPa)	73.6	67.6	61.6	56
Sample type	C PPA100	C PPHA50	C PPHA40	C PPHA30
Stress Values (MPa)	70.2	64.2	59	51.4

As the percentage of natural dammar resin increased, the values of compressive breaking strength exhibited a downward trend. This decrease can be attributed to the fact that dammar resin inherently has lower resistance to mechanical stresses compared to synthetic resins, such as epoxy or acrylic, which provide better structural cohesion and superior rigidity. In contrast, the analysis of the results revealed an increase in compression displacement as the proportion of dammar in the matrix composition increased. This behavior can be explained by the greater elasticity of natural dammar resin compared to synthetic resins, resulting in an enhanced ability of the material to deform before failure. Thus, it can be concluded that a higher dammar content promotes increased ductility in the specimens, influencing their mechanical response. These findings are essential for optimizing material composition, allowing for the adjustment of the ratio between natural and synthetic components based on the specific requirements of the intended applications. If the goal is to manufacture a material with high elasticity, and strength is not a primary concern, then specimens with the highest possible percentage of dammar are preferred (such as those in the C PPE30 or C PPA30 categories). However, if strength is a key factor while also ensuring environmental friendliness, it is recommended to use materials containing an equal ratio of 50% to 50% dammar and synthetic resin.

By comparing the results of the present research with similar findings from the literature, higher values were observed than those reported by Wang and Long (2021). This can be explained by the fact that pine needles provide better adhesion when integrated into composite materials compared to when they are used in concrete production. A possible explanation could be that concrete does not fully cover the surface around the material, leading to voids during the casting process—voids that could be interpreted as material defects and stress concentrators, potentially causing the specimens to break at much lower stresses than in a real-case scenario.

An enhanced compressive strength—approximately 1.8 times higher—was reported by Cogurcu (2022) for composites reinforced with pine needles. This improvement may be attributed to the pre-treatment process applied to the pine needles, which involved immersion in a 5% sodium hydroxide solution before incorporation into the matrix. Additionally, the use of polycarboxylic ether (in concentrations ranging from 1.60% to 2.50%) as a plasticizing agent during the manufacturing of the composite likely contributed to the superior mechanical performance.

Bending Test

In the bending tests, a procedure similar to that used for tensile and compression tests was applied, ensuring the comparability of the results. The characteristic force-displacement curves obtained for the representative specimens from each material set are illustrated in Fig. 7, providing a detailed perspective on their mechanical behavior. These data are essential for assessing the strength and deformability of the analyzed materials.

The results confirm the trends observed in previous destructive tests, highlighting differences between the tested materials. Specifically, the maximum forces at which specimen fracture occurred were considerably higher for those with an epoxy resin-based matrix compared to those containing acrylic resin. This difference can be attributed to the superior mechanical properties of epoxy resin, which provides increased resistance to mechanical stresses, whereas acrylic resin exhibits structurally and mechanically inferior characteristics.

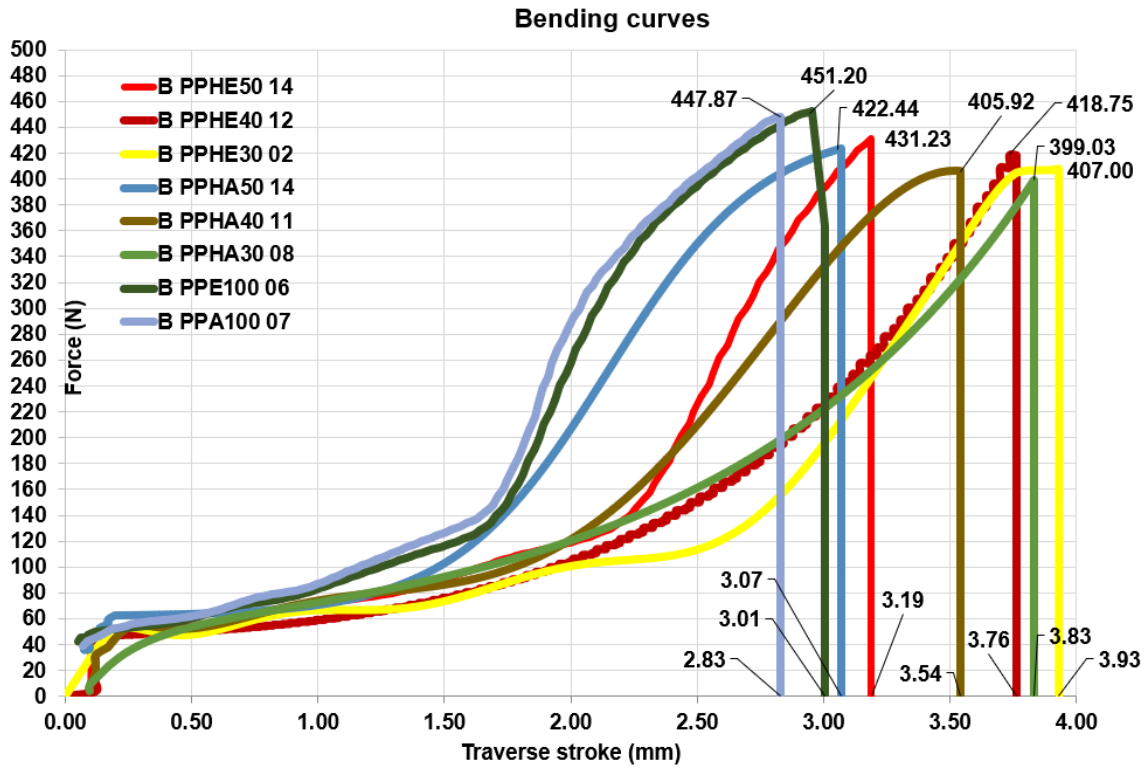

Fig. 7. The force-displacement curves from the bending test for the representative samples, with a matrix from all 8 types of resins

Furthermore, the analysis of the influence of the dammar percentage on the mechanical behavior of the tested materials revealed a clear trend: as the dammar concentration increased, the maximum breaking force decreased, indicating a reduction in bending strength. Simultaneously, the traverse stroke increases, signaling an improvement in the material's elasticity. This phenomenon can be explained by the more flexible nature of dammar resin compared to synthetic resins, which, although enhancing ductility, led to a reduction in rigidity and, consequently, the material's ability to withstand intense mechanical loads.

The arithmetic mean values for bending strength, presented in Table 5, confirm this trend, showing a progressive decrease in breaking strength as the dammar percentage

increases. This behavior can be explained by the weaker mechanical properties of natural dammar resin, which, while providing greater flexibility, reduced the material's capacity to endure high mechanical loads. These findings are essential for understanding the effect of matrix composition on the mechanical performance of the tested materials and can contribute to optimizing the use of natural resins in specific applications.

Table 5. Arithmetic Mean Values for the Bending Breaking Strength Values

Sample Type	B PPE100	B PPHE50	B PPHE40	B PPHE30
Stress Values (MPa)	42.3	40.4	39.2	
Sample Type	B PPA100	B PPHA50	B PPHA40	B PPHA30
Stress Values (MPa)	41.9	39.5	38	

From the perspective of flexural performance, the present study recorded higher values compared to those reported by Cogurcu (2022). In fact, the thermal treatment applied to the pine needles—consisting of immersion in a 5% sodium hydroxide solution prior to matrix integration—appeared to have no beneficial effect under bending stress; on the contrary, it may have even contributed to a reduction in these properties. When compared to the findings of Sinha *et al.* (2018), the mechanical performance observed in this research was lower, with values approximately 1.9 times smaller.

Vibration Test

For vibration analysis, the specimens were firmly clamped at one end using a vice, which was positioned on a solid table to ensure the necessary stability during the experiment. Each specimen was tested using free lengths of 100, 120, 140, 160, and 180 mm, allowing for a detailed assessment of structural behavior depending on the length of the free segment. To determine the damping characteristics of the system, the logarithmic decrement method was applied, a technique commonly used in structural dynamic analysis. The damping factor was calculated based on the mathematical relationship specified in Eq. 1, ensuring an accurate evaluation of energy dissipation in the tested material (Mirițoiu 2024):

$$\mu = \frac{1}{t_2 - t_1} \cdot ln \frac{v_2}{v_1} \quad (1)$$

Equation 1 considers the time values associated with two successive peaks of the oscillation, denoted as t_1 and t_2, extracted from the amplitude diagram. Additionally, it incorporates the corresponding peak amplitudes at these time points, designated as v_1 and v_2, allowing for a detailed assessment of how the oscillation amplitude decreases over time. These values are essential for determining the damping characteristics of the system and analyzing the vibrational behavior of the tested material. For a better understanding of the results, Fig. 8 presents the obtained values for the damping factor and natural frequency specific to the vibrations of the V PPHA30 sample. These data provide a clear insight into the material's ability to dissipate mechanical energy and its response to external excitations. Thus, analyzing these parameters contributes to a more precise characterization of the dynamic properties of the tested specimen.

Figures 9 and 10 illustrate the results obtained from the vibration test, focusing on the relationship between the damping factor and the free length of the specimens, as well as the correlation between natural frequency and free length. Through analyzing these graphical representations, a clear trend can be observed: both the natural frequency and the

damping factor decrease progressively as the free length of the specimens increases. This phenomenon suggests that the size of the free segment of the material directly influences the vibrational behavior of the specimens, leading to reduced energy dissipation and a decrease in system stiffness as the length increases. One of the main explanations for the variations observed in natural frequency values among the different specimens is the difference in the mechanical properties of the materials used, particularly regarding the elastic modulus. Materials with a higher elastic modulus tend to exhibit higher natural frequencies, indicating better resistance to deformation and increased stiffness. Conversely, materials with a lower elastic modulus, such as those based on acrylic resin, show lower natural frequencies, which translates into a reduced ability to return to their original state after mechanical excitation.

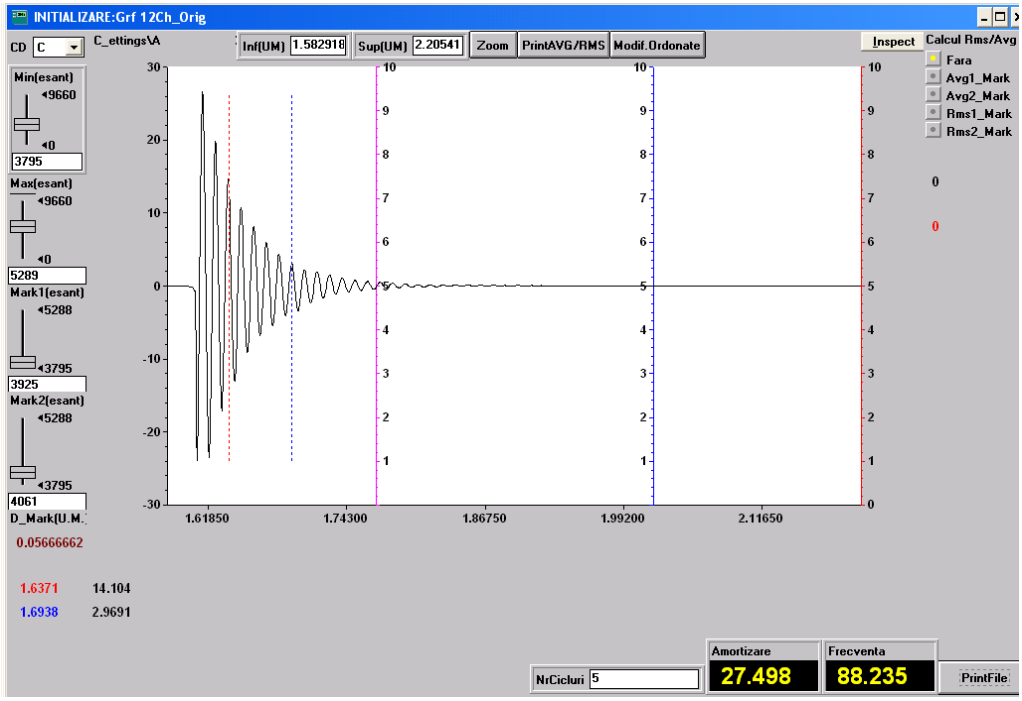

Fig. 8. Vibration monitoring, including the damping factor and natural frequency, for the V PPHA30 specimen with a free length of 140 mm

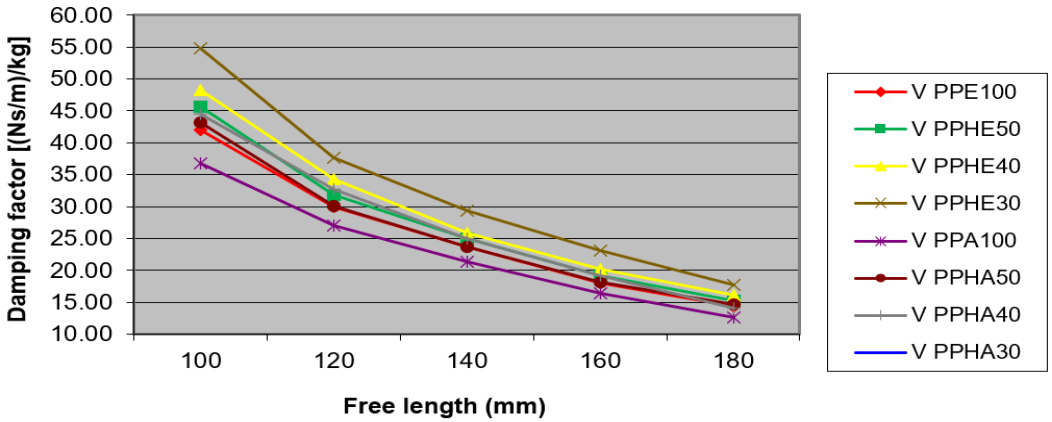

Fig. 9. Analysis of the damping factor in relation to the free length of the specimens for all the samples

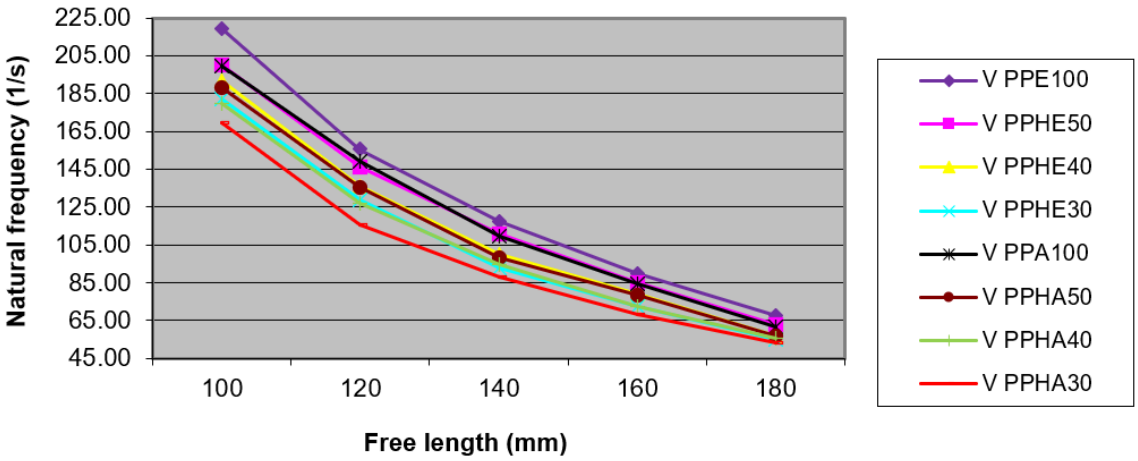

Fig. 10. Data obtained from the vibration test regarding the natural frequency for all the samples

A clear distinction can be observed between specimens made of acrylic resin (V PPA) or bio-based resin with an acrylic component (V PPHA50, V PPHA40, V PPHA30) and those made of epoxy resin or bio-based resins with an epoxy component. The acrylic-based specimens exhibited both lower natural frequencies and lower damping factors compared to those made with epoxy-based resins. This result can be attributed to the inferior mechanical properties of acrylic resin compared to epoxy resin, which provides greater stiffness and a better ability to maintain structural integrity under mechanical stress. Supporting this observation, tensile tests provided additional data confirming the influence of resin type on the mechanical behavior of the specimens. The results showed that specimens containing epoxy resin or a bio-based system with an epoxy component exhibited higher breaking strength and greater elongation at break compared to those based on acrylic. This difference is significant because it indicates that epoxy resin not only improves the stiffness of the material but also contributes to better mechanical resistance, which explains the higher natural frequencies and better damping behavior observed in vibration tests. Another important aspect highlighted by the analysis of Fig. 10 is the influence of the natural dammar resin content on the vibration damping capacity. Specimens containing a higher percentage of dammar demonstrated a superior ability to dissipate vibrational energy. This phenomenon can be explained by the increased elasticity of the material as the proportion of dammar resin rises. As the material's elasticity improves, vibrations are attenuated more quickly, leading to more effective oscillation damping. This conclusion is also supported by destructive tests conducted on the materials, which indicated a direct correlation between the percentage of dammar in the matrix composition and the increase in material elasticity. Thus, as the dammar content increased, the material became more flexible, contributing to a faster attenuation of vibrations and a decrease in natural frequency. In conclusion, the variations in natural frequency observed among the specimens were closely related to differences in the elastic modulus of the materials used. Specimens made from acrylic resin or bio-based resins with an acrylic component exhibited lower natural frequencies and damping factors compared to epoxy-based specimens. This trend can be explained by the inferior mechanical properties of acrylic resin, which is also reflected in the results of tensile tests, where specimens containing epoxy resin or bio-based with epoxy part demonstrated superior breaking

strength and greater elongation at break compared to those made from acrylic materials. Therefore, the choice of resin type used in the material composition, influences its vibrational and mechanical characteristics and incorporating a higher percentage of dammar can contribute to more effective vibration damping by increasing the material's elasticity. In comparison with similar vibration studies, an increase was observed in both the natural frequency and the damping factor. The word *similar* was used because both in the present study and in the reference Miritoiu (2024), the same experimental setup and equipment were used for measuring and recording free vibrations. The equipment and experimental setup were detailed in the current research in the section *Test Standards and Characterizations*, under the subsection *Vibration test*. The similarities with the study by Miritoiu (2024) also include the paper support onto which biomass residues were applied. The difference between the two studies lies in the type of biomass residues used: chicken feathers in Miritoiu (2024) and pine needles in the present research. This behavior can be explained by the superior vibrational properties of pine needles compared to chicken feathers, especially considering that the other components of the composite materials remained unchanged (see Miritoiu (2024)).

Shore D Hardness Test

The values obtained from the Shore hardness test, using the D scale, are presented in Fig. 11. A clear decreasing trend in Shore D hardness values was observed as the percentage of dammar resin increased. This trend can be attributed to the influence of dammar resin, which enhances the elasticity of the specimens, making them less rigid and more flexible. As a result, the ability of the material to resist indentation was reduced, leading to lower hardness values. Furthermore, the analysis of Fig. 11 highlighted that specimens containing epoxy resin in the matrix exhibited higher Shore D hardness compared to those incorporating acrylic resin. This difference can be explained by the superior mechanical properties of epoxy resin, which provides greater resistance to deformation and increased structural integrity. In contrast, acrylic resin contributes to a softer and more flexible material, resulting in lower hardness values. These findings align with previous observations regarding the mechanical behavior of the tested materials, further reinforcing the idea that the type and composition of the resin play a crucial role in determining the overall hardness and elasticity of the specimens.

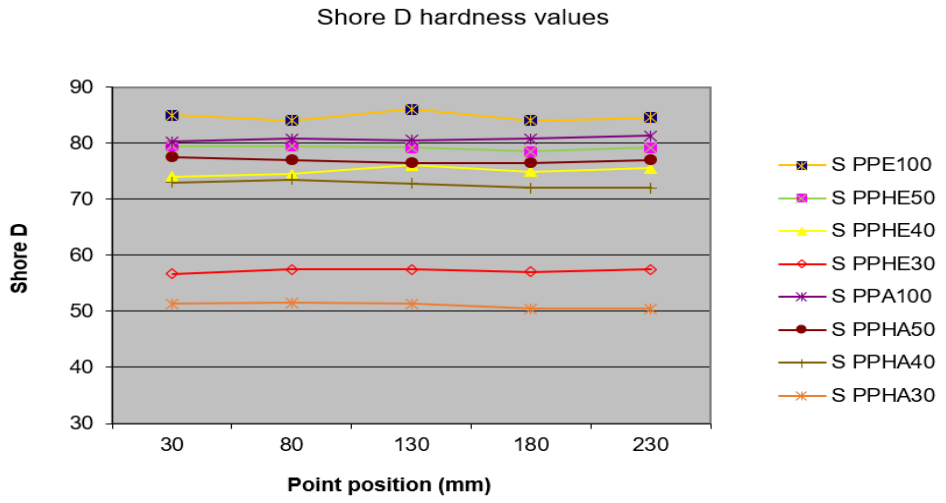

Fig. 11. Experimental data regarding the measured Shore D hardness values

The rigidity of a material represents its ability to resist deformation under the action of an external force. The less the material deforms under a given load, the higher its rigidity. In Shore hardness tests, this property is evaluated by measuring the penetration depth of an indenter into the surface of the material using a gauge mounted on a durometer. Harder materials exhibit greater resistance to penetration, meaning that they can more effectively counteract the force applied by the indenter due to their internal structure. Analyzing the relationship between rigidity and hardness, a clear correlation between these two properties was observed. For example, in tensile tests, all analyzed specimens had the same cross-sectional area, allowing for an objective comparison between them. The rigidity of these materials is largely determined by their elastic modulus values. Materials with a higher elastic modulus exhibit increased rigidity, meaning they resist both axial deformation under tensile stress and indentation penetration during the Shore hardness test. Comparing the values obtained for Shore hardness and tensile strength, this phenomenon was confirmed: materials with a higher elastic modulus also had higher Shore D hardness values, while materials with a lower elastic modulus exhibited lower hardness. The incorporation of natural dammar resin into the polymer matrix influenced the mechanical properties of the materials. An increase in the percentage of dammar resin led to greater elasticity, which was reflected in a decrease in tensile strength and an increase in elongation at break. This indicates a reduction in the overall rigidity of the material and, consequently, a decrease in its hardness. The same trend was observed in the Shore D hardness values. As the material's ductility increased, its ability to resist indenter penetration decreased, leading to lower hardness values. Lower Shore hardness values indicate a softer material that is more easily penetrated and more flexible under applied force. Because all tested specimens were reinforced using the same type of reinforcement, the observed differences in hardness can primarily be attributed to variations in the composition of the bio-based resins and the influence of the dammar resin percentage on the final mechanical properties of the material. Thus, the results suggest that the choice of resin composition plays a crucial role in determining the material's rigidity and hardness. Increasing the proportion of dammar resin results in a more flexible material with lower hardness, whereas using a resin with a high elastic modulus, such as epoxy resin, provides greater hardness and rigidity. These findings are essential for applications where an optimal balance between flexibility and indentation resistance is required, such as in the composite materials and technical polymer industries. When compared to the results reported by Ma *et al.* (2014), the current study revealed a slightly reduced hardness—approximately 1.1 times lower. This outcome can plausibly be linked to the surface modification protocol employed in their research, which involved an initial immersion of the fibers in a 1:1 solution of benzene and formaldehyde for 24 hours, followed by treatment with 2% sodium hydroxide for 2 hours, thorough rinsing with water, and a final wash using a 1 wt% sulfuric acid solution.

Water Absorption Results

Figure 12 provides a detailed presentation of all experimental results regarding the water absorption capacity of the tested materials.

In the first phase, the water absorption was tested for all types of resins presented in Table 1. It was found that they were insoluble in water, with no water absorption. In the next stage, the reinforced samples with paper waste and pine needles trash were immersed, using the eight types of matrices presented in Table 1. The samples exhibited an almost constant daily rate of water absorption throughout the testing period. This phenomenon was primarily attributed to the presence of paper in the material's composition, given that

all other components of the matrix, whether synthetic or bio-based, were found to be completely insoluble in water. It is well known that paper consists largely of cellulose, a highly hydrophilic substance, which explains the material's tendency to retain water. Due to its chemical nature, cellulose can attract and retain water molecules, leading to an increase in the composite's mass when exposed to humid environments or immersed in water. This behavior has also been reported and confirmed in the scientific literature, including studies conducted by Adhikary *et al.* (2008) and Tsai *et al.* (2001), which highlighted the influence of cellulosic materials on water absorption in fiber-based composites. Thus, the obtained results support the idea that water absorption in these composites is primarily determined by the presence of paper, with the hydrophilic nature of cellulose playing a crucial role in this process.

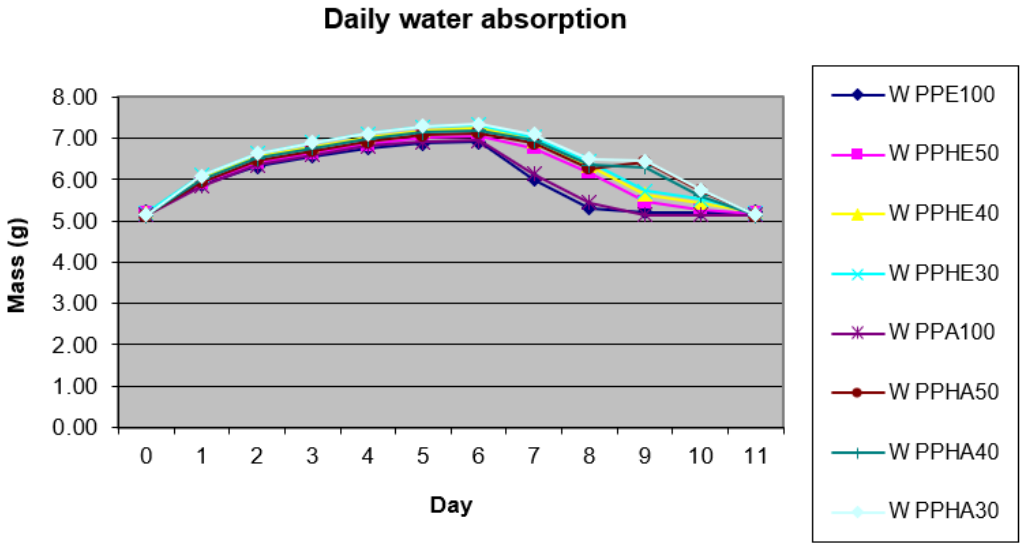

Fig. 12. Daily water absorption

On the 6th day of the experiment, it was observed that the mass difference of the samples, compared to the 5th day, was small, with a maximum value of 0.05 g. This slight variation indicated that the water absorption process had reached a saturation point, and the tested materials were no longer accumulating an amount of water. Therefore, it was considered that the water absorption experiment could be concluded, as no further relevant changes in the mass of the samples were recorded. After completing the absorption test, the samples were left to dry at room temperature without being subjected to any artificial drying process. This step was necessary to allow the materials to gradually release the accumulated water and return to their initial mass. The drying process was monitored daily to observe the behavior of the samples in contact with the ambient air. Starting from the 7th day, a progressive decrease in the mass of the samples was observed, indicating that the water absorbed over the previous six days had begun to evaporate. As the water retained within the material's structure evaporated, the samples continued to lose mass until they reached their initial equilibrium, thus confirming that the water absorption process was reversible under the established experimental conditions.

It was found that the samples with a matrix composed entirely of 100% synthetic resins returned to their initial mass in a shorter time compared to those containing natural dammar resin. This phenomenon can be explained by the differences in chemical

composition and hygroscopic behavior between synthetic and natural resins. Synthetic resins are generally characterized by a more stable chemical structure and lower moisture absorption, which allows for faster elimination of retained water during the experiment. In contrast, natural dammar resin, being an organic material derived from plant sources, exhibits higher porosity and a greater capacity to retain water compared to synthetic resins. As a result, the samples containing dammar required a longer time to fully eliminate the accumulated water and return to their initial mass. These findings suggest that the nature of the matrix directly influences both the water absorption rate and the subsequent drying process. The samples with synthetic resins exhibited a more hydrophobic behavior, facilitating faster water evaporation, while those containing natural resin displayed a more hygroscopic behavior, requiring a longer time for complete drying. The thickness swelling test was not considered in the current study. However, it will be given priority in a future continuation of the research.

Compared to other studies, it can be observed that water absorption reached the saturation point much faster, specifically in 6 days, compared to 9 days as found in the study by Miritoiu (2024), where composite materials reinforced with paper waste and chicken feathers were investigated. This can be explained by the fact that, although pine needles contain cellulose and hemicellulose in a proportion of 80% (Alzebdeh *et al.* 2019; Cogurcu 2022), the presence of 15% lignin reduces water access to the internal structure because lignin is hydrophobic. Additionally, the wax, resins, and pectin that make up the remaining 5% form a natural water-repellent barrier on the surface. Another possible reason is that the pine needles used were green, meaning they already contained water within their tissues, making them less capable of absorbing additional water from the external environment. Furthermore, another possible explanation is that green pine needles are active photosynthetic organs adapted to regulate water exchange through stomata. They can limit external water absorption by closing their stomata and maintaining controlled internal pressure.

CONCLUSIONS

1. Dammar-based resins represent a viable option for use as a matrix in the manufacturing of sustainable composite materials reinforced with paper waste and pine needles; these matrices provide both suitable mechanical properties and good compatibility with natural fibers, making them ideal for eco-friendly applications.
2. The paper waste and pine needles contribute to improving the rigidity and strength of the composite materials.
3. Following the destructive tests conducted, the composite materials exhibited satisfactory mechanical properties, indicating an effective adhesion between the bio-based matrix which has dammar in composition and the reinforcing material; good compatibility between these components is essential for ensuring a uniform distribution of mechanical stresses and preventing delamination or other structural defects.
4. The bond between the bio-based matrix which has dammar in composition and reinforcement was good, otherwise the resulting mechanical properties would have been lower, affecting tensile, flexural or compression strength; this would have considerably limited the practical use of these materials in engineering applications, where durability and reliability are crucial.

5. The addition of dammar resin to the synthetic resin composition causes it to act as a plasticizer, making the matrix softer, but the incorporation of cellulosic reinforcements helped compensate for the decrease in the elastic modulus of the matrix caused by the presence of dammar resin.
6. The experimental results show that increasing the proportion of dammar resin from 50% up to 70%, led to lower strength but higher elongation at break (higher plasticity), indicating a shift toward more ductile behavior due to the resin's softer, more elastic nature compared to synthetic resins.
7. The experimental results confirm that the use of dammar-based resins can provide adequate mechanical performance, making these composites suitable for various structural and functional applications (such as furniture parts, interior decorations and so on).
8. The experimental results suggest that the presence of dammar resin has a beneficial effect on the material's ability to dissipate mechanical energy, making it promising for applications that require effective vibration damping.
9. The water absorption was lower compared to other composite materials because pine needles contain lignin, wax, resins, and pectin, which act as a natural water-repellent barrier on the surface.

REFERENCES CITED

Abdel-Ghani, M., Edwards, H. G. M., Stern, B., and Janaway, R. (2009). "Characterization of paint and varnish on a medieval Coptic-Byzantine icon: Novel usage of dammar resin," *Spectrochimica Acta Part A* 73, 566-575. DOI: 10.1016/j.saa.2008.10.050

Adhikary, K. B., Pang, S., and Staiger, M. P. (2008). "Long-term moisture absorption and thickness swelling behaviour of recycled thermoplastics reinforced with *Pinus radiata* sawdust," *Chemical Engineering Journal* 142(2), 190-198. DOI: 10.1016/j.cej.2007.11.024

Alzebdeh, K. I., Nassar, M. M. A., and Arunachalam, R. (2019). "Effect of fabrication parameters on strength of natural fiber polypropylene composites: Statistical assessment," *Measurement* 146, 195-207. DOI: 10.1016/j.measurement.2019.06.012

Asghar, A., Raman, A. A. A., and Daud, W. M. A. W. (2014). "A comparison of central composite design and Taguchi method for optimizing the Fenton process," *The Scientific World Journal* 2014, article ID 869120. DOI: 10.1155/2014/869120

ASTM D570-22 (2022). "Standard test method for water absorption of plastics," ASTM International, West Conshohocken, PA, USA.

ASTM D695 (2016). "Standard test method for compressive properties of rigid plastics," ASTM International, West Conshohocken, PA, USA.

ASTM D790-17 (2017). "Standard test methods for flexural properties of unreinforced and reinforced plastics and electrical insulating materials," ASTM International, West Conshohocken, PA, USA.

ASTM D2240-17 (2021). "Standard test method for rubber property—Durometer hardness," ASTM International, West Conshohocken, PA, USA.

ASTM D3039 (2014). "Standard test method for tensile properties of polymer matrix

composite materials," ASTM International, West Conshohocken, PA, USA.
Azmat, H. (2024). "Converting pine needles from a fire risk into a livelihood opportunity," *Mongabay-India*, (https://india.mongabay.com/2024/04/converting-pine-needles-from-a-fire-risk-into-a-livelihood-opportunity/), Accessed 04 Feb 2025.
Bisht, A. S., and Thakur, N. S. (2020). "Pine needles biomass gasification-based electricity generation for the Indian Himalayan region: Drivers and barriers," in: *Green Building and Sustainable Engineering*, Springer, Berlin, Germany, pp. 47-59.
Bonaduce, I., Odlyha, M., Di Girolamo, F., Lopez-Aparicio, S., Grøntoft, T., and Colombini, M. P. (2013). "The role of organic and inorganic indoor pollutants in museum environments in the degradation of dammar varnish," *Analyst* 138, 487-500. DOI: 10.1039/c2an36259g
Chung, D., Lee, J.-H., Lee, S.-Y., Park, K.-W., and Shim, K.-Y. (2021). "Efficacy of pine needles as bioindicators of air pollution in Incheon, South Korea," *Atmospheric Pollution Research* 12 (5), article ID 101063. DOI: 10.1016/j.apr.2021.101063.
Ciucă, I., Stănescu, M. M., Bolcu, D., Mirițoiu, C. M., and Rădoi, A. I. (2022). "Study of mechanical properties for composite materials with hybrid matrix based on dammar and natural reinforcers," *Environmental Engineering and Management Journal* 21(2), 299-307
Clarocit Kit. (2023). "ClaroCit Kit, 800 g powder, 500 mL liquid and required consumables," (https://webshop.struers.com/en/product/40200072), accessed 7 September 2023
Clearfield, A. (2000). "Inorganic ion exchangers, past, present and future," *Solvent Extraction and Ion Exchange* 18(4), 655-678. DOI: 10.1080/07366290008934702
Cogurcu, T. M. (2022). "Investigation of mechanical properties of red pine needle fiber reinforced self-compacting ultra high-performance concrete," *Case Studies in Construction Materials* 16, article ID e00970. DOI: 10.1016/j.cscm.2022.e00970
Dickens, D., Morris, L., Clabo, D., and Ogden, L. (2020). "Pine straw raking and growth of southern pine: Review and recommendations," *Forests* 11(8), article 799. DOI: 10.3390/f11080799
Dinesh, B. K., and Kim, J. (2023). "Mechanical and dynamic mechanical behavior of lignocellulosic pine needle fiber-reinforced SEBS composites," *Polymers* 15(5), article 1225. DOI: 10.3390/polym15051225
Duryea, M. L. (1989). "Pine straw management in Florida's forests," *Florida Cooperative Extension Service, Institute of Food and Agricultural Sciences, University of Florida*, CIR 831, (https://ufdcimages.uflib.ufl.edu/IR/00/00/18/18/00001/FR07800.pdf), Accessed 4th of February 2025.
Dyer, J. F., Barlow, R. J., Kush, J. S., and Gilbert, J. C. (2012). "Pine straw production: From forest to front yard," *Proceedings of the 16th Biennial Southern Silvicultural Research Conference*, Charleston, SC, USA, pp. 100–108
Flemingfarm (2017). "Gathering pine needles for animal winter bedding," *Steemit*, (https://steemit.com/homesteading/@flemingfarm/gathering-pine-needles-for-animal-winter-bedding), Accessed 06 Feb 2025
Foita de Aur. (2023). "Foita de aur. Magazin materiale de pictura," (https://foitadeaurmagazin.ro/), accessed 5 September 2023
Franz, M. H., Neda, I., Maftei, C. V., Ciucă, I., Bolcu, D., and Stănescu, M. M. (2021). "Studies of chemical and mechanical properties of hybrid composites based on natural resin dammar formulated by epoxy resin," *Polymer Bulletin* 78, 2427-2438.

DOI: 10.1007/s00289-020-03221-4

Fu, Y., Cheng, Y., Chen, C., Li, D., and Zhang, W. (2022). "Study on preparation process and enhanced piezoelectric performance of pine-needle-like ZnO@PVDF composite nanofibers," *Polymer Testing* 108, article ID 107513. DOI: 10.1016/j.polymertesting.2022.107513

Gairola, S., Gairola, S., Sharma, H., and Rakesh, P. K. (2019). "Impact behavior of pine needle fiber/pistachio shell filler-based epoxy composite," *Journal of Physics: Conference Series* 1240, article ID 012096. DOI: 10.1088/1742-6596/1240/1/012096

Ghosh, M. K., and Ghosh, U. K. (2011). "Utilization of pine needles as bed material in solid-state fermentation for the production of lactic acid by *Lactobacillus* strains," *BioResources* 6(2), 1556-1575. DOI: 10.15376/biores.6.2.1556-1575

Gresham, C. A. (1982). "Litterfall patterns in mature loblolly and longleaf pine stands in coastal South Carolina," *Forest Science* 28(2), 223–231.

Guo, Y., Huang, S., Zhao, L., Zhang, J., Ji, C., and Ma, Q. (2022). "Pine (*Pinus massoniana* Lamb.) needle extract supplementation improves performance, egg quality, serum parameters, and the gut microbiome in laying hens," *Frontiers in Nutrition* 9, article ID 810462. DOI: 10.3389/fnut.2022.810462

Gupta, S., and Mondal, P. (2021). "Catalytic pyrolysis of pine needles with nickel-doped gamma-alumina: Reaction kinetics, mechanism, thermodynamics, and product analysis," *Journal of Cleaner Production* 286, article ID 124930. DOI: 10.1016/j.jclepro.2020.124930

Gupta, A., Kumar, V., Preetam, A., and Kumar, M. (2023). "A novel combinatorial approach for cleaner production of biodegradable sheets from the combination of paddy straw and pine needle waste," *Journal of Cleaner Production* 421, article ID 138440. DOI: 10.1016/j.jclepro.2023.138440

Gupta, S., Patel, P., and Mondal, P. (2022). "Biofuels production from pine needles via pyrolysis: Process parameters modeling and optimization through a combined RSM and ANN-based approach," *Fuel* 310(Part A), article ID 122230. DOI: 10.1016/j.fuel.2021.122230

Houghton, R. A. (2008). "Biomass," in: *Encyclopedia of Ecology*, S. E. Jørgensen and B. D. Fath (eds.), Academic Press, Oxford, UK, pp. 448-453.

International Panel on Climate Change (IPCC) (2011). *Renewable Energy Sources and Climate Change Mitigation. Special Report of the Intergovernmental Panel on Climate Change*, IPCC, Cambridge, New York, NY, USA.

IQ Economy+. (2024). "Hartie copiator A3 IQ Economy+ 80 g/mp 500 coli/top," (https://www.bnb.ro/hartie-copiator-a3-iq-economy-80-g-mp-500-coli-top.html), accessed 5 February 2024

Khan, T. (2012). "How an Uttarakhand company is producing electricity with pine needles," *Business Today*, (https://www.businesstoday.in/magazine/features/story/uttarakhand-company-producing-power-with-pine-needles-35270-2012-12-19), Accessed 05 Feb 2025.

Khuller, A. (2019). "Fuel from forests," *Renewable Watch*, (https://renewablewatch.in/2019/09/20/fuel-from-forests/), Accessed 06 Feb 2025.

Kingsbury, D. (2025). "How to use and repurpose pine needles for home and garden," *Reuse, Repurpose, Save*, (https://www.reuse-repurpose-save.com/post/how-to-use-and-repurpose-pine-needles-for-home-and-garden), Accessed 06 Feb 2025.

Klánová, J., Čupr, P., Baráková, D., Šeda, Z., Anděl, P., and Holoubek, I. (2009). "Can pine needles indicate trends in the air pollution levels at remote sites?,"

Environmental Pollution 157(12), 3248-3254. DOI: 10.1016/j.envpol.2009.05.030

Koutsaviti, A., Toutoungy, S., Saliba, R., Loupassaki, S., Tzakou, O., Roussis, V., and Ioannou, E. (2021). "Antioxidant potential of pine needles: A systematic study on the essential oils and extracts of 46 species of the genus *Pinus*," *Foods* 10(1), article 142. DOI: 10.3390/foods10010142

La Nasa, J., Degano, I., Modugno, F., and Colombini, M. P. (2014). "Effects of acetic acid vapour on the ageing of alkyd paint layers: Multi-analytical approach for the evaluation of the degradation processes," *Polymer Degradation and Stability* 105, 257-264. DOI: 10.1016/j.polymdegradstab.2014.04.010

Likus-Cieślik, J., Socha, J., Gruba, P., and Pietrzykowski, M. (2020). "The current state of environmental pollution with sulfur dioxide (SO_2) in Poland based on sulfur concentration in Scots pine needles," *Environmental Pollution* 258, article ID 113559. DOI: 10.1016/j.envpol.2019.113559

Long, W., and Wang, Y. (2021). "Effect of pine needle fibre reinforcement on the mechanical properties of concrete," *Construction and Building Materials* 278, article ID 122333. DOI: 10.1016/j.conbuildmat.2021.122333

Ma, Y., Liu, Y., Shang, W., Gao, Z., Wang, H., Guo, L., and Tong, J. (2014). "Tribological and mechanical properties of pine needle fiber reinforced friction composites under dry sliding conditions," *RSC Advances* 4, 36777-36783. https://pubs.rsc.org/en/content/articlelanding/2014/ra/c4ra06717g

Mahajan, R., Chandel, S., Puniya, A. K., and Goel, G. (2020). "Effect of pretreatments on cellulosic composition and morphology of pine needle for possible utilization as substrate for anaerobic digestion," *Biomass and Bioenergy* 141, article ID 105705. DOI: 10.1016/j.biombioe.2020.105705

Maleki, A., Jafari, A. A., and Yousefi, S. (2017). "Green cellulose-based nanocomposite catalyst: Design and facile performance in aqueous synthesis of pyranopyrimidines and pyrazolopyranopyrimidines," *Carbohydrate Polymers* 175, 409-416. DOI: 10.1016/J.CARBPOL.2017.08.019

Malkapuram, R., Kumar, V., and Negi, Y. S. (2010). "Novel treated pine needle fiber reinforced polypropylene composites and their characterization," *Journal of Reinforced Plastics and Composites* 29(15), 2343-2355. DOI: 10.1177/073168440934

Mirițoiu, C. M., Stănescu, M. M., and Bolcu, D. (2020). "Research regarding the mechanical properties of a new hybrid vegetal resin," *Materiale Plastice* 57(1), 37-45. DOI: 10.37358/Mat.Plast.1964

Mirițoiu, C. M. (2024). "Mechanical properties of composite materials with dammar-based matrices and reinforced with paper and chicken feathers waste," *BioResources* 19(3), 4698-4717. DOI: 10.15376/biores.19.3.4698-4717

Miritoiu, C. M. (2024). "Influence of dammar resin on the mechanical properties of composites reinforced with corn husk and paper waste," *BioResources* 19(4), 9416-9446. DOI: 10.15376/biores.19.4.9416-9446

Mittal, H., Kaith, B. S., and Jindal, R. (2010). "Synthesis, characterization and swelling behaviour of poly (acrylamide-co-methacrylic acid) grafted gum ghatti based superabsorbent hydrogels," *Advances in Applied Science Research* 1(3), 56-66.

Operato, L., Vitiello, L., Aprea, P., Ambrogi, V., Salzano de Luna, M., and Filippone, G. (2023). "Life cycle assessment of poly(lactic acid)-based green composites filled with pine needles or kenaf fibers," *Journal of Cleaner Production* 387, article ID 135901. DOI: 10.1016/j.jclepro.2023.135901

Polydis. (2023). "Polydis," (https://polydis.ro/), accessed 7 September 2023
Rana, A. K., Guleria, S., Gupta, V. K., and Thakur, V. K. (2023). "Cellulosic pine needles-based biorefinery for a circular bioeconomy," *Bioresource Technology* 367, article ID 128255. DOI: 10.1016/j.biortech.2022.128255
Resoltech 1050. (2023). "Resoltech 1050. Hardeners 1053s to 1059s. Structural lamination epoxy system," (https://www.resoltech.com/en/markets/1050-detail.html), accessed 7 September 2023
Singha, A. S., and Jyoti, A. (2013). "Mechanical, morphological, and thermal properties of chemically treated pine needles reinforced thermosetting composites," *Journal of Applied Polymer Science* 127, 387-393. DOI: 10.1002/app.37636
Singha, A. S., and Thakur, V. K. (2008). "Mechanical, morphological, and thermal properties of pine needle-reinforced polymer composites," *International Journal of Polymer Materials and Polymer Biomaterials* 58(1), 21-31. DOI: 10.1080/00914030802461857
Singha, A. S., and Thakur, V. K. (2010). "Synthesis, characterization and study of pine needles reinforced polymer matrix based composites," *Journal of Reinforced Plastics and Composites* 29(5), 644-656. DOI: 10.1177/0731684408100354
Sinha, P., Mathur, S., Sharma, P., and Kumar, V. (2018). "Potential of pine needles for PLA-based composites," *Polymer Composites* 39(4), 1339-1349. DOI: 10.1002/pc.24074
Soong, J. L., Parton, W. J., Calderon, F., Campbell, E. E., and Cotrufo, M. F. (2015). "A new conceptual model on the fate and controls of fresh and pyrolized plant litter decomposition," *Biogeochemistry* 124, 27-44. DOI: 10.1007/s10533-015-0079-2
Stănescu, M. M. (2015). "A study regarding the mechanical behaviour of Dammar based composite materials, reinforced with natural fiber fabrics," *Materiale Plastice* 52(4), 596-600.
Struers. (2023). "Struers GmbH, Sucursala Bucuresti (România)," (https://www.struers.com/), accessed 7 September 2023
Strzałkowski, J., Kampragkou, P., Stefanidou, M., Horszczaruk, E., and Głowacka, A. (2024). "Lavender and black pine waste as additives enhancing selected mechanical and hygrothermal properties of cement mortars," *Materials* 17(22), article 5475. DOI: 10.3390/ma17225475
Taylor, E. L., and Foster, C. D. (2004). "Producing pine straw in East Texas forests," *Texas Cooperative Extension*, Publication B-6145, Laredo, TX, USA.
Thakur, V. K., and Singha, A. S. (2011). "Physicochemical and mechanical behavior of cellulosic pine needle-based biocomposites," *International Journal of Polymer Materials and Polymer Biomaterials* 16(6), 390-398. DOI: 10.1177/073168440934
Thakur, V. K., Singha, A. S., and Thakur, M. K. (2013). "Fabrication and physico-chemical properties of high-performance pine needles/green polymer composites," *International Journal of Polymer Materials and Polymer Biomaterials* 62(4), 226-230. DOI: 10.1080/00914037.2011.641694
Third Pole (2017). "Fires ravage forests in Himalayas, threatening health and biodiversity," *The Third Pole*, (https://www.thethirdpole.net/en/climate/fires-ravage-forests-himalayas-threatening-health-biodiversity/), Accessed 06 Feb 2025.
Topp, N. E., and Pepper, K. W. (1949). "Properties of ion-exchange resins in relation to their structure, Part I. Titration curves," *Journal of the Chemical Society* 690, 3299-3303.
Tsai, W. T., Chang, C. Y., Wang, S. Y., Chang, C. F., Chien, S. F., and Sun, H. F. (2001).

"Cleaner production of carbon adsorbents by utilizing agricultural waste corn cob," *Resources, Conservation and Recycling* 32(1), 43-53. DOI: 10.1016/S0921-3449(00)00093-8

Vestgarden, L. S., Nilsen, P., and Abrahamsen, G. (2004). "Nitrogen cycling in *Pinus sylvestris* stands exposed to different nitrogen inputs," *Scandinavian Journal of Forest Research* 19(1), 38-47. DOI: 10.1080/02827580310019572

Wang, Y., and Long, W. (2021). "Complete stress–strain curves for pine needle fibre reinforced concrete under compression," *Construction and Building Materials* 302, article ID 124134. DOI: 10.1016/j.conbuildmat.2021.124134

Xie, J., Yang, Z., Feng, Y., Chen, H., Hu, L., Jia, J., and Wu, D. (2022). "Optimization of the extraction process of pine needle essential oil by response surface methodology and its chemical composition analysis," *BioResources* 17(4), 5890-5904. DOI: 10.15376/biores.17.45890-5904

Zsigmond, A. R., Száraz, A., and Urák, I. (2021). "Macro and trace elements in black pine needles as inorganic indicators of urban traffic emissions," *Environmental Pollution* 291, article ID 118228. DOI: 10.1016/j.envpol.2021.118228

Article submitted: March 3, 2025; Peer review completed: March 29, 2025; Revised version received and accepted: March 31, 2025; Published: April 8, 2025.
DOI: 10.15376/biores.20.2.3884-3909